

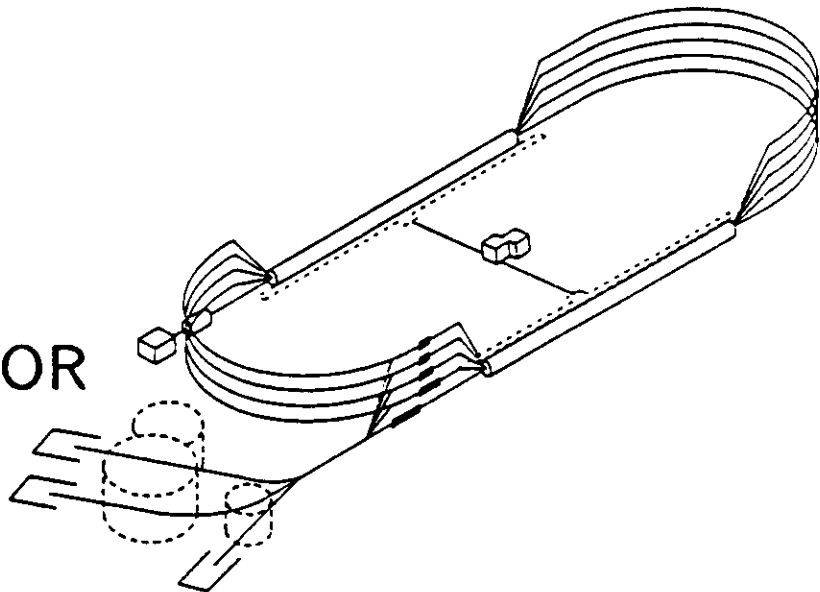
HADRON PHYSICS AT THE NEW CW ELECTRON ACCELERATORS

Volker D. Burkert

Continuous Electron Beam Accelerator Facility,
Newport News, Virginia 23606, USA

Invited talk presented at the Rheinfels Workshop 1990 Hadron Mass Spectrum,
St. Goar, Germany, September 3 - 6, 1990.

C O N T I N U O U S E L E C T R O N B E A M A C C E L E R A T O R F A C I L I T Y



SURA SOUTHEASTERN UNIVERSITIES RESEARCH ASSOCIATION

CEBAF

Newport News, Virginia

Copies available from:

Library
CEBAF
12000 Jefferson Avenue
Newport News
Virginia 23606

The Southeastern Universities Research Association (SURA) operates the Continuous Electron Beam Accelerator Facility for the United States Department of Energy under contract DE-AC05-84ER40150.

DISCLAIMER

This report was prepared as an account of work sponsored by the United States government. Neither the United States nor the United States Department of Energy, nor any of their employees, makes any warranty, express or implied, or assumes any legal liability or responsibility for the accuracy, completeness, or usefulness of any information, apparatus, product, or process disclosed, or represents that its use would not infringe privately owned rights. Reference herein to any specific commercial product, process, or service by trade name, mark, manufacturer, or otherwise, does not necessarily constitute or imply its endorsement, recommendation, or favoring by the United States government or any agency thereof. The views and opinions of authors expressed herein do not necessarily state or reflect those of the United States government or any agency thereof.

HADRON PHYSICS AT THE NEW CW ELECTRON ACCELERATORS

Volker D. Burkert

Continuous Electron Beam Accelerator Facility,
12000 Jefferson Avenue, Newport News, Virginia 23606, USA

Major trends of the physics program related to the study of hadron structure and hadron spectroscopy at the new high current, high duty cycle electron machines are discussed. It is concluded that planned experiments at these machines may have important impact on our understanding of the strong interaction by studying the internal structure and spectroscopy of the nucleon and lower mass hyperon states.

1. INTRODUCTION.

In the past decades intermediate energy electromagnetic interactions have been employed to study the structure of hadrons using elastic electron scattering, and photo- and electroproduction of mesons. Most of these experiments have covered rather limited kinematic regimes, because of low rates and the use of detectors and magnetic spectrometers with small solid angle and momentum acceptance. This was dictated by the background generated by an intense, low duty cycle electron beam interacting with an external target. This situation limited the usefulness of the electromagnetic probe in studies of hadron structures and hadron spectroscopy. For example, of the about 25 well established excited nucleon states not a single one was discovered using electron or photon beams, albeit many states were found to have large photocoupling amplitudes. With the construction and partial completion of several new CW electron accelerators this situation is changing significantly. Firstly, use of large acceptance detectors at high luminosities of $10^{34} \text{ cm}^{-2} \text{ sec}^{-1}$ will become feasible, allowing measurement of several reaction channels simultaneously, over a large kinematic range, and with statistical accuracy comparable to that achieved with hadronic probes. Secondly, with 100% duty cycle intense electron beams, high resolution and high statistics coincidence measurements can be conducted for exclusive channels with small cross sections, e.g. pion production off nucleons near threshold. In fact, data rates will to a large degree not be limited by the luminosity achievable in these measurements but rather by the data collection speed of the data acquisition system. It is interesting to note that this situation eliminates the traditional 'rate advantage' of hadronic reactions over

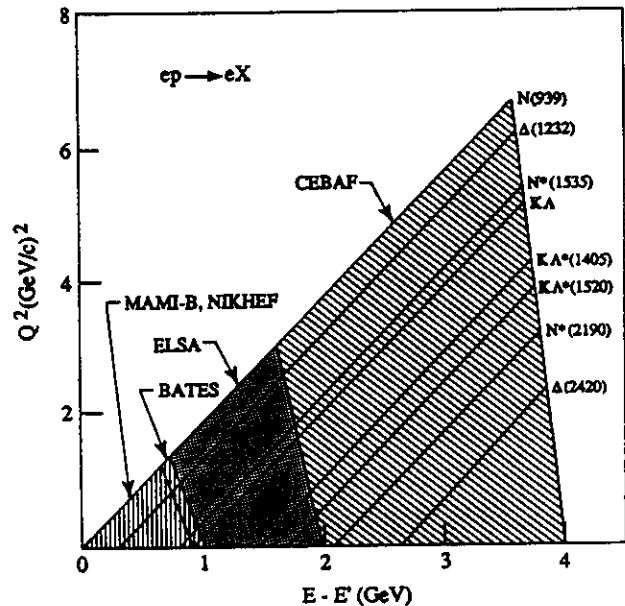


Figure 1.1 Kinematic domains accessible at various DC electron accelerators.

electromagnetic processes. Electromagnetic processes may hence be studied with statistical sensitivity similar to hadronic reactions. This will bring to bear the full capability of the electromagnetic interaction as a probe of the internal structure of hadrons.

A variety of DC machines are presently under construction (NIKHEF, MIT-Bates, CEBAF), or are near-

ing completion (ELSA-Bonn, MAMI-Mainz). Some important machine parameters are listed in table 1.1. An

Parameter	MAMI-B	NIKHEP	MIT-Bates	ELSA	CEBAF
Energy [GeV]	0.85	0.9	1.0	2.0/3.5	4.0
$\delta E/E$	10^{-4}	$2 \cdot 10^{-3}$	$0.4 \cdot 10^{-3}$	10^{-3}	10^{-4}
I(ext) [μA]	100	40	50	0.2	200
I(int) [mA]	-	200	80	50	-
duty factor	1.0	0.9	0.85	0.95/0.2	1.0
completion	1990	1992	1992	1988	1994

energy range from a few hundred MeV up to 4 GeV will be accessible when all machines are fully operational. The scientific programs at the various laboratories span a broad range of physics topics from the more traditional nuclear physics aspects related to the interaction of hadrons in nuclei, to studies of the structure of free hadrons and their modifications in the nuclear medium. Correspondingly diverse is the experimental equipment that will be needed in order to fully exploit the capabilities of the machines, and to span the broad scientific programs.

In this talk I focus on aspects of the scientific programs that are directly related to the topics discussed at this workshop - the excitation and internal structure of hadrons in free space. The kinematical domains accessible with the various accelerators in electron nucleon scattering are shown in Figure 1.1.

2. STRUCTURE OF THE NUCLEON

Interest in the structure of the nucleon and its excited states has dramatically increased in recent years and is one of the major motivations in support of the planned experimental program at the new electron machines. The structure of the nucleon may be probed in elastic electron nucleon scattering and in inelastic reactions induced by electrons and photons. These studies are of fundamental importance since they measure the charge and current distribution as well as the transition currents of the fundamental building blocks of matter. Knowledge of these quantities allows stringent tests of microscopic models applicable at low and intermediate energies, such as QCD based quark models, chiral bag models, Skyrme models, etc.. Near the pion production

threshold the validity of low energy theorems (LET) can be tested. At very high energies, the transition from the non-perturbative to the perturbative regime can be studied, where simple quark counting rules may apply.

2.1 Electromagnetic Formfactors.

The hadronic current in elastic electron nucleon scattering is specified by the electric and magnetic formfactors $G_E(Q^2)$ and $G_M(Q^2)$. These are related to the Dirac and Pauli formfactors F_1 and F_2 as:

$$G_E = F_1 - \tau F_2, \quad G_M = F_1 + F_2$$

where $\tau = \frac{Q^2}{4M^2}$. The usual techniques for measuring the elastic formfactors is the Rosenbluth separation, where one makes use of the different angular dependence of the electric and the magnetic term in the unpolarized elastic cross section to separate $|G_E|$ and $|G_M|$

$$\frac{d\sigma}{d\Omega} = \left(\frac{d\sigma}{d\Omega}\right)_M \frac{E'}{E} [(G_E^2 + \tau G_M^2) + 2\tau(1 + \tau)G_M^2 \tan^2 \frac{\theta}{2}].$$

This techniques ceases to be useful, when either $G_E^2 \ll G_M^2$, or at high values of Q^2 , where the magnetic contributions dominate both the angular dependent and the angular independent terms.

Experimental information on the neutron electric formfactor G_{En} is rather poor for all non-zero Q^2 . In the absence of a free neutron target, we have to rely on scattering from the few-nucleon systems. Unlike for the proton, the Rosenbluth separation of G_{En} from G_{Mn} is difficult even at low Q^2 because of the small size of G_{En} compared to G_{Mn} . At low Q^2 , G_{En} would be non-zero only if the charge distribution within the neutron were not uniform. The slope of G_{En} versus Q^2 , at low Q^2 has been accurately measured, and it is positive, indicating that the neutron appears to have a slightly positive core surrounded by a region of negative charge. For $Q^2 < 1 \text{ GeV}^2$ G_{En} has been extracted from elastic electron-deuteron scattering data^{1,2}. Using this procedure, however, it is necessary to assume a model for the deuteron structure which renders the extraction of G_{En} model dependent. The result of the most recent analysis is shown in Figure 2.1. Clearly, model independent data, and data at higher Q^2 are needed for an unambiguous confrontation with various model calculations. The electric formfactor of the proton has been measured at SLAC³ using Rosenbluth separation for Q^2 up to about 4 GeV^2 , with error bars of 20% at the highest momentum transfer. The proton magnetic formfactor has been measured for Q^2 up to 31 GeV^2 . An analysis of the electromagnetic formfactors by Gari and Stefanis⁴ allowed extraction of the QCD scale parameter Λ_{QCD} .

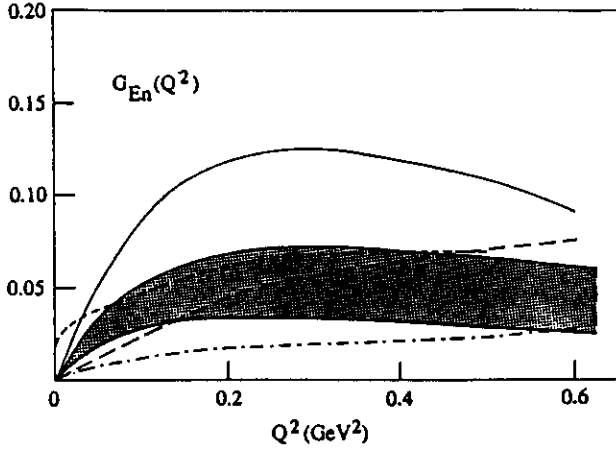


Figure 2.1 The electric formfactor G_{E_n} of the neutron extracted from elastic electron deuteron scattering². The shaded area indicates the uncertainty due to the choice of the deuteron wavefunction. The curves are results of model calculations: Chiral Bag Model⁴⁰ (dashes), Relativized Quark Model²³ (solid), RQM⁵¹ (dotted), Skyrme Model⁵² (short dashes).

In lowest order, Λ_{QCD} can be defined in relation to the strong coupling constant α_s :

$$\alpha_s(Q^2) = \frac{12\pi}{(33 - 2n_f) \ln(Q^2/\Lambda_{QCD}^2)}$$

where n_f is the number of quarks with mass lower than Q^2 . Assuming a conventional meson picture at small Q^2 , and asymptotic QCD predictions at high Q^2

$$F_1 = \frac{C_1}{Q^4}, \quad F_2 = \frac{C_2}{Q^6},$$

(modulo powers of $\ln(Q^2/\Lambda_{QCD})$) the fit to the electromagnetic formfactors (Figure 2.2) yielded values for Λ_{QCD} between 100 to 250 MeV/c. The uncertainties are mainly due to the limited knowledge of G_{E_p} at $Q^2 \geq 2 \text{ GeV}^2$. A more precise determination of this parameter will be very interesting since Λ_{QCD} is not well constrained by other measurements⁴⁴.

2.2 Polarization Techniques to Measure G_E .

Two methods appear very promising in the measurement of G_{E_n} in a model independent fashion. Both methods employ quasi elastic scattering of polarized electrons off deuterium. In the first case polarized electrons are scattered off polarized deuterium⁵. In the second case an unpolarized deuterium target is used and the polarization of the recoil neutron is measured in a second scattering experiment⁶. The two methods are

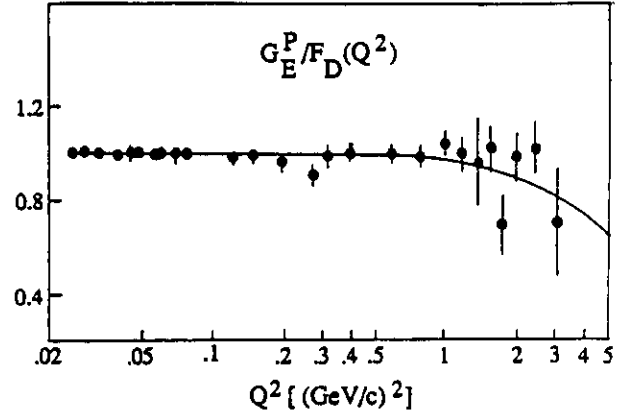


Figure 2.2 Result of the QCD analysis of the proton elastic formfactors⁴ using $\Lambda = 180 \text{ MeV}$. The solid line represents the fit to the data.

equivalent, and allow measurement of the polarization asymmetry

$$A_{en} = \frac{2\tau \cos\theta'_T + 2\sqrt{2\tau(1+\tau)} \cdot (G_{E_n}/G_{M_n}) \sin\theta \cos\phi v'_{TL}}{v_L(1+\tau)(G_{E_n}/G_{M_n})^2 + 2\tau v_T}$$

where v_L, v_T, v'_T, v'_{TL} are known kinematical quantities. By varying θ , the angle between the nuclear spin and the direction of momentum transfer, it is possible to pick out the longitudinal and transverse pieces of the quasi elastic spin dependent cross section. In particular, if $\theta = 90^\circ$, the asymmetry is proportional to G_{E_n}/G_{M_n} . If G_{M_n} is known, G_{E_n} can be determined.

The first method uses a polarized ($N\bar{D}_3$)^{7,8,9} or $^3\bar{H}e$ ¹⁰ target, in an external electron beam. If the polarization asymmetry is measured using vector polarized deuterium, it will be necessary to measure the recoil neutron in coincidence with the scattered electron to veto against the much larger asymmetry effects due to the polarized proton in the deuteron. Model calculations¹¹ show (Figure 2.3) that the polarization asymmetry is linearly dependent on G_{E_n}/G_{M_n} as long as the recoil neutron is emitted at small angles with respect to the direction of the virtual photon. In this region the influence of the deuteron wave function on the extracted value of G_{E_n}/G_{M_n} is almost absent. A quantitative check can be accomplished by measuring the proton asymmetry at the same time, and by comparing it to the asymmetry obtained with a polarized hydrogen target (e.g. $N\bar{H}_3$). For $^3\bar{H}e$, nuclear corrections are not negligible¹² and have to be carefully studied if G_{E_n} is to be extracted.

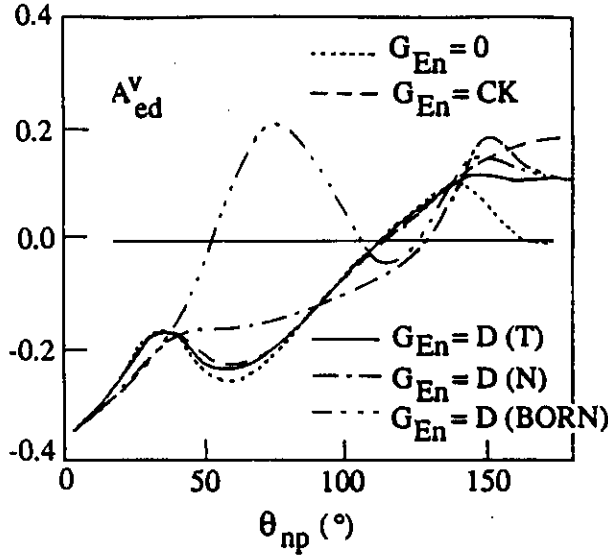


Figure 2.3 Double polarization asymmetry A_{ed}^v for different G_{En} , and various interaction models¹⁵.

Employing state-of-the-art polarized target technology it appears feasible to measure G_{En} for Q^2 up to 0.5 GeV^2 with a 1 GeV electron beam, and up to 2 or 3 GeV^2 using a 4 GeV beam. Projected error bars for a measurement at CEBAF which employs the recoil polarization techniques are shown in Figure 2.4. Likely, the first precise data in the lower Q^2 range will come from measurements in preparation at MAMI-B¹⁰.

The polarization techniques discussed above can also be used to measure the electric formfactor G_{Ep} of the proton. Recoil polarization techniques using an unpolarized hydrogen target¹³, and the measurement using a polarized $N\bar{H}_2$ target¹⁴ appear most promising. With a 4 GeV beam, values of Q^2 up to 5 GeV^2 and error bars less than 5% can be reached with either techniques. Recent advances in polarized target technology¹⁵ may allow one to push this limit to even higher values.

2.3 Pion Photoproduction at Threshold

For many years the low energy theorems (LET) for pion production at threshold have been viewed as solid achievements of theoretical physics. The assertion of LET is that in the low energy limit the process is determined by calculating the Born terms, and using vector current conservation and the PCAC hypothesis. In this case the isospin amplitudes take on a very simple form:

$$A^- = 1, \quad A^{+,0} = -\frac{1}{2}\mu + \frac{1}{4}\mu^2\mu^{v,s},$$

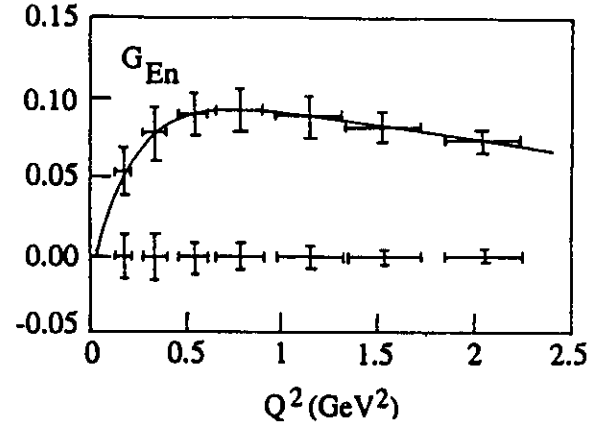


Figure 2.4 Projected data for a measurement of G_{En} at CEBAF using recoil polarization techniques¹⁵.

$$\mu^{v,s} = \mu_p \mp \mu_n, \quad \mu = \frac{m_\pi}{M_N}$$

The isospin amplitudes for pion production are given by:

$$A(\gamma p \rightarrow \pi\pi^+) = \sqrt{2}(A^- + A^0)$$

$$A(\gamma n \rightarrow p\pi^-) = \sqrt{2}(A^- - A^0)$$

$$A(\gamma p \rightarrow p\pi^0) = (A^+ + A^0)$$

$$A(\gamma n \rightarrow n\pi^0) = (A^+ - A^0)$$

allowing absolute predictions of cross sections at threshold. For the charged pion processes the LET predictions agree well with the measurements. However, recent π^0 measurements at Saclay¹⁶ and Mainz¹⁷ showed that the LET predictions were almost an order of magnitude higher than the data.

Nath and Singh¹⁸ proposed that chiral symmetry breaking in QCD due to final quark masses give another contribution to LET. Tiator et al.¹⁹ argued that isospin symmetry breaking in QCD, which is responsible for the mass difference $\delta m = m_u - m_d \simeq -3.8 \text{ MeV}$ should give yet another contribution to the LET. With these QCD corrected LET, an excellent agreement with the data is obtained (Figure 2.5). If this interpretation of the LET corrections holds, threshold pion production might offer the possibility of more precise determination of the u and d quark masses. The prediction for the dominant E_{0+} multipole is shown in table 2.1. The $\gamma n \rightarrow n\pi^0$ process has not been measured at threshold, however, assuming isoscalar and isovector ($\Delta I = 0, 1$) transitions only, the amplitudes can be predicted from the other measurements. Direct measurements of this channel should yield smaller error bars, allowing a more definite comparison with theoretical predictions. Independent measurement of this process would also allow determination of upper limits of possible isotensor contributions, for which there is presently no experimental

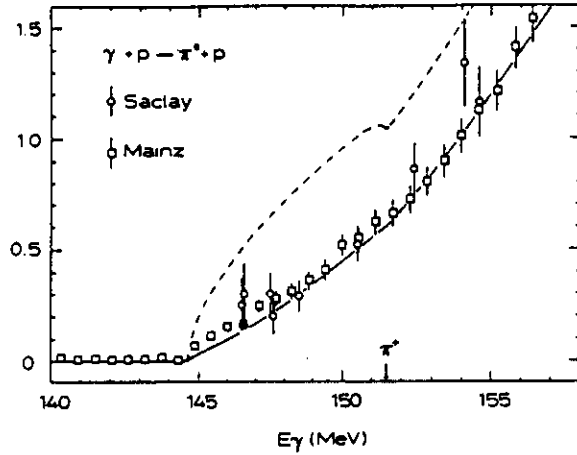


Figure 2.5 Cross section data for π^0 photoproduction off protons near threshold compared to LET predictions without (dashed) and with (solid) corrections for quark mass effects¹⁹

evidence. Note that in the absence of isotensor contributions only the ISB calculation is in agreement with the data.

Extension to pion electroproduction should prove extremely interesting, as possible violation of LET can be studied for the different spatial regions probed with increasing Q^2 . Electron scattering measurements are planned at MAMI and MIT-Bates.

Table 2.1: MULTIPOLE E_{0+} AT THRESHOLD					
Channel	LET	CQM	CSB	ISB	Experiment
$\gamma p \rightarrow \pi \pi^+$	27.5	29.0	28.7 ± 0.3	28.7 ± 0.3	$28.3 \pm 0.5^{[20]}$
$\gamma n \rightarrow \pi \pi^-$	-32.0	-33.3	-30.8 ± 0.3	-30.8 ± 0.3	$-31.9 \pm 0.5^{[21]}$
$\gamma p \rightarrow \pi \pi^0$	-2.4	-2.7	0.0 ± 0.7	-0.8 ± 0.5	$-0.5 \pm 0.3^{[26]}$
					$-0.35 \pm 0.1^{[27]}$
$\gamma n \rightarrow \pi \pi^0$	0.4	0.4	1.1 ± 0.2	1.6 ± 0.4	(2.2 ± 0.4)

2.3 Pion Electroproduction at Threshold

The differential cross section for charged pion electroproduction at threshold is s -wave dominated. Beside the electric monopole transition multipole E_{0+} it contains only the longitudinal multipole L_{0+} :

$$\frac{d\sigma}{d\Omega} = \frac{W|p_\pi^*|}{E_\gamma M} [|E_{0+}|^2 + \epsilon Q^2 |L_{0+}|^2]$$

Within the framework of current algebra theory and PCAC, E_{0+} is sensitive to the axial vector formfactor G_A via the contact interaction, and the electromagnetic

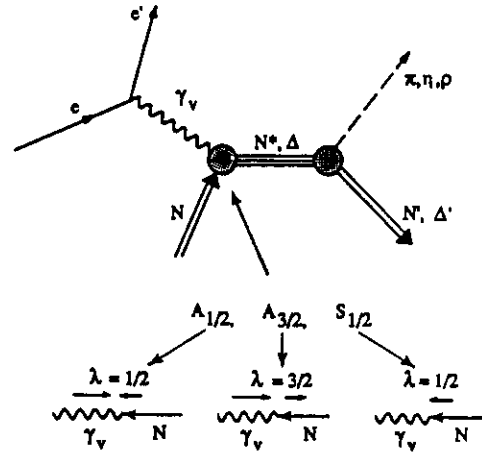


Figure 2.6 Electroproduction of hadronic final states via s -channel resonance decays. The γNN^* vertex is described by the photocoupling helicity amplitudes $A_{1/2}$, $A_{3/2}$, $S_{1/2}$.

nucleon formfactors. At threshold, E_{0+} is proportional to G_A . The two terms in the cross section can be determined experimentally by measuring the ϵ dependence. Using $G_A(Q^2)$ as derived from charged current neutrino reactions, the validity of LET versus Q^2 can be tested by inspection of E_{0+} . Alternatively, assuming the validity of LET for charged pion production, $G_A(Q^2)$ can be extracted from the data. L_{0+} is essentially a function of G_{E_N} and the pion formfactor F_π . Since $G_{E_N}(Q^2)$ will be measured in independent experiments, $F_\pi(Q^2)$ can be extracted from the data. At low Q^2 the model dependence of this procedure can be tested by comparing the extracted values of F_π with direct measurements in elastic πe scattering. If the model dependence can be understood, extension of this procedure to higher Q^2 may then become possible. It is worth noting that the high Q^2 data on F_π comes exclusively from analyses of unseparated electroproduction cross section measurements. They presently contain a model dependence which may be largely eliminated in future experiments.

2.4 Baryon Resonance Transition Formfactors.

A large number of resonances, attributed to the excitation of the nucleon have been observed in hadron scattering, the $\Delta(1232)$ being the most prominent one. Electroexcitation of resonances on the free nucleon yields information on the $\gamma_N NN^*$ vertex as a function of Q^2 (Figure 2.6). The transition into a specific excited state is described by three amplitudes $A_{1/2}(Q^2)$, $A_{3/2}(Q^2)$, and $S_{1/2}(Q^2)$, where A and S refer to transverse and scalar coupling, respectively, and the subscripts refer to the total helicity of the $\gamma_N N$ system.

Inclusive measurement of $\gamma N \rightarrow X$, or $eN \rightarrow eX$ reveal a few broad bumps, clearly indicating the excitation of resonances in the mass region below 2 GeV. Their broad widths and close spacing makes it impossible to separate them in inclusive production reactions. By explicit measurement of the decay products such as $\pi N, \eta N, \rho N, \pi \Delta$, and others, it is possible to identify them according to their spin and isospin assignments. The experimental status of light quark baryon states and their electromagnetic transitions is discussed in detail in another contribution to this conference²².

The physics issues one hopes to study are manifold, and address fundamental questions about the interaction of quarks and gluons in confined systems. Specifically, one would like to study how the transition between the 3-quark ground state and excited states is mediated. Most models assume that the excitation is due to a single quark transition. However, recent studies²³ indicate that double quark transitions may be present at a non-negligible level. Measurement of the Q^2 evolution of the transition formfactors provides information about the wave function of the excited state. The helicity asymmetry

$$A_{1/2,3/2} = \frac{A_{1/2}^2 - A_{3/2}^2}{A_{1/2}^2 + A_{3/2}^2}$$

for the transition into excited states as the $D_{13}(1520)$ or $F_{15}(1688)$ was found to be sensitive to the potential that confines the valence quarks inside the nucleon²³. At high momentum transfer, one may observe the transition from the non-perturbative to the perturbative regime, where power law rules for the helicity amplitudes are predicted to apply²⁴ such that:

$$A_{1/2} = C_1/Q^3, \quad A_{3/2} = C_2/Q^5, \quad Q^2 \rightarrow \infty$$

if logarithmic terms are neglected. Whether this regime can be reached at the available energies (e.g. 4 GeV at CEBAF) is an open question. Nonetheless, it will be interesting to push studies of the helicity structure of nucleon resonance excitations to the highest possible Q^2 . The QCD motivated extension of the non-relativistic quark model²⁵ predicts many states, in particular at higher masses, which have not been observed in πN reactions. Theoretical calculations²⁶ indicate that the "missing" states tend to decouple from the πN channel but couple strongly to $N\rho, N\omega$, and $\Delta\pi$. This would explain why they have not been seen in elastic πN scattering. Our picture of baryon structure could drastically change if these states did not exist. Several of these states are predicted to couple strongly to photons (real or virtual) and may thus be searched for in photo- or electroproduction experiments. Experiments to search for these states in multi pion production are

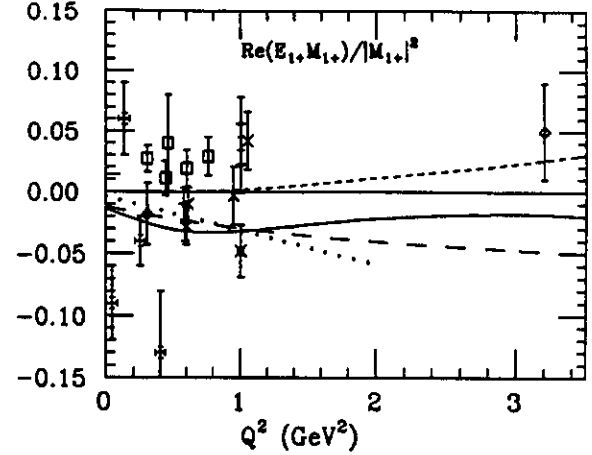


Figure 2.7 Comparison of experimental data on the interference term $Re(E_{1+}, M_{1+})/|M_{1+}|^2$ for the $\Delta(1232)$ with various model calculations.

in preparation at ELSA and CEBAF. A complete program to study nucleon resonance transitions, e.g. in $\gamma_e N \rightarrow \pi N$, involves measurement of 6 (4 in photoproduction) complex, parity conserving amplitudes.

$$H_i := \langle \lambda_\pi; \lambda_N | T | \lambda_\gamma; \lambda_p \rangle = \langle 0; \pm \frac{1}{2} | T | \pm 1, 0; \pm \frac{1}{2} \rangle$$

which makes it necessary to measure at least 11 independent observables, not counting additional measurements to resolve quadratic ambiguities. Experiments involving unpolarized particles only, allow measurement of only 4 response functions $\sigma_T, \sigma_L, \sigma_{TT}, \sigma_{LT}$:

$$\frac{d\sigma}{d\Omega} = \sigma_T + \epsilon\sigma_L + \epsilon\sigma_{TT}\cos 2\phi + \sqrt{2\epsilon(1+\epsilon)}\sigma_{LT}\cos\phi,$$

$$\sigma_i = \sigma_i(H_1, \dots, H_6)$$

Measurement of polarization observables yields information on many response functions. For example, with a polarized electron beam, and a polarized nucleon target 14 more response functions can be measured.

I want to illustrate the significance of polarization measurements for this program with two examples, the transitions $\gamma_e p \Delta^+(1232)$, and $\gamma_e p P_{11}^+(1440)$.

2.4.1 The Transition $\gamma_e p \rightarrow \Delta^+(1232) \rightarrow N\pi$.

In SU(6) symmetric quark models, this transition is explained by a simple quark spin-flip in the $L_{3Q} = 0$ ground state, corresponding to a magnetic dipole transition M_{1+} . The electric and scalar quadrupole transitions are predicted to be $E_{1+} = S_{1+} = 0$. In more elaborate QCD based models which include color magnetic interactions arising from the one-gluon exchange at small distances, the $\Delta(1232)$ acquires an $L_{3Q} = 2$

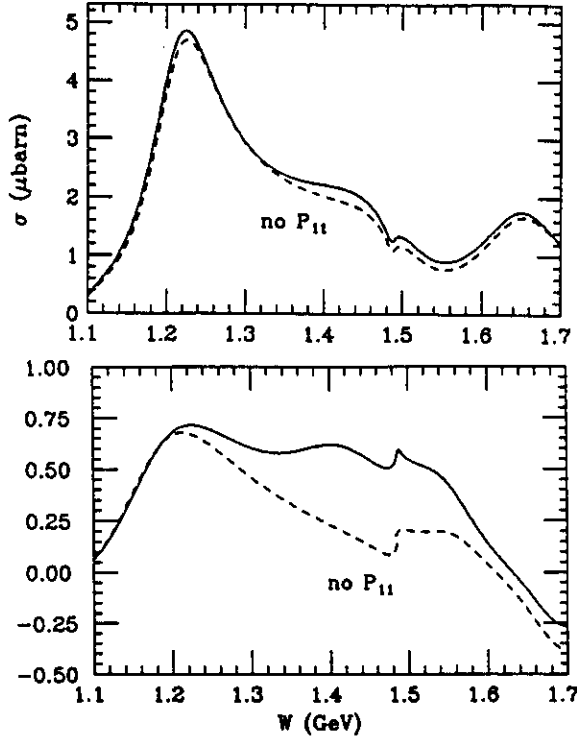


Figure 2.8 Predicted cross section for $\gamma_p p \rightarrow p\pi^0$ at $Q^2 = 1\text{GeV}^2$, $\epsilon = 0.8$, $\theta_\pi^* = 0.$, using the amplitudes of G. Kroesen³⁰. The sensitivity to the (small) amplitudes of the Roper resonance is shown (top). Predicted target asymmetry T_n for the same kinematics (bottom).

component, leading to small electric and scalar contributions (e.g. $|E_{1+}/M_{1+}| \simeq 0.01$ at $Q^2 = 0$). The ratio $|E_{1+}/M_{1+}|$ is predicted to be weakly dependent on Q^2 . At very high Q^2 , QCD predicts²⁷ $E_{1+}/M_{1+} \rightarrow 1$, and $S_{1+}/M_{1+} \rightarrow 0$. Precise measurements of these contributions from $Q^2 = 0$ to very large Q^2 are obviously important for the development of realistic models of the nucleon. Present experimental information about E_{1+} is shown in Figure 2.7, together with model predictions. The quality of the data is clearly not sufficient to discriminate against any of the models. Experiments at MIT-Bates²⁸ and CEBAF²⁹ are in preparation to measure the electric and scalar quadrupole transition over a large Q^2 range, using polarized electron beams and/or recoil polarimeters. In these experiments one obtains information about the terms

$$M_{1+}, \text{Re}(E_{1+}M_{1+}^*), \text{Re}(S_{1+}M_{1+}^*),$$

$$\text{Im}(E_{1+}M_{1+}^*), \text{Im}(S_{1+}M_{1+}^*).$$

The imaginary parts of the bilinear terms can only be accessed using polarization degrees of freedom. They

are particularly sensitive to phase relations between the multipoles. If the multipoles were strictly in phase, these terms would vanish identically.

2.4.2 The Transition $\gamma_p p \rightarrow P_{11}^+(1440) \rightarrow N\pi$.

The Roper resonance P_{11} has a modestly strong photocoupling at $Q^2 = 0$, but in electron scattering there is little evidence for its excitation both in the inclusive cross section and in exclusive single pion production at $Q^2 < 1\text{GeV}^2$. In an analysis³⁰ of single pion production data at $Q^2 = 1\text{GeV}^2$, a small positive value was found for the $A_{1/2}(P_{11})$ amplitude. At $Q^2 = 0$ this value is larger and negative. One may speculate that the apparent quenching of the Roper at $Q^2 > 0$ might be accidental and related to a zero crossing of the transverse amplitude. The P_{11} may then be expected to "reappear" at higher Q^2 . In fact, non-relativistic as well as relativized quark models predict³¹ the $A_{1/2}(P_{11})$ amplitude to grow relative to the $\Delta(1232)$. In non-relativistic models $A_{1/2}(P_{11})/A_{1/2}(\Delta) \sim \bar{Q}^2$, so that the P_{11} would dominate at high Q^2 .

It has been pointed out that the dominance of the P_{11} at high Q^2 will be a crucial test of the quark model classification as a $N=2$ radially excited state³². Measurements with polarized proton targets¹⁴, or proton recoil polarization measurements³³ can provide a strong signature for the excitation of this resonance in electron scattering experiments. Figure 2.8 shows the sensitivity of the unpolarized cross section and the polarized target asymmetry T_n in $\gamma_p p \rightarrow p\pi^0$ to the P_{11} amplitudes. Clearly, measurement of polarization observables will have an important impact on the determination of the photocoupling amplitudes of the Roper.

3. PARITY VIOLATION EXPERIMENTS.

At low and medium energy ($Q^2 \ll M_Z^2$) neutral current interactions, the parity violating contributions arise from the interference between the one-photon exchange and the neutral weak boson Z^0 exchange graphs (Figure 3.1). In electron scattering the interaction contains an isoscalar as well as an isovector piece in both the vector (V_μ) and the axial vector (A_μ) coupling. The relevant piece of the Lagrangian can be written as

$$L_{pv} = \frac{G_F}{\sqrt{2}} \cdot [\bar{e}\gamma_\mu\gamma_5 e(\bar{\alpha}V_\mu^3 + \bar{\gamma}V_\mu^0) + \bar{e}\gamma_\mu e(\bar{\beta}A_\mu^3 + \bar{\delta}A_\mu^0)]$$

where $\bar{\alpha}$, $\bar{\beta}$, $\bar{\gamma}$, $\bar{\delta}$ denote the electro-weak coupling constants. In the Standard Model the coupling constants are related to the weak mixing angle θ_W in the following way:

$$\bar{\alpha} = -(1 - \sin^2\theta_W), \quad \bar{\beta} = -(1 - 4\sin^2\theta_W),$$

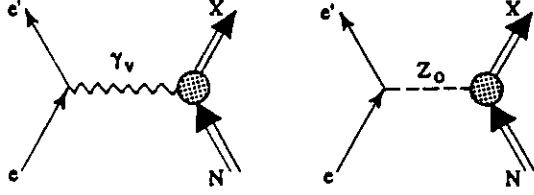


Figure 3.1 Lowest order Feynman diagrams which contribute to parity non-conservation in electron scattering at low and intermediate energies.

$$\tilde{\gamma} = \frac{2}{3} \sin^2 \theta_W, \quad \tilde{\delta} = 0,$$

where $\sin^2 \theta_W = 0.232 \pm 0.004$.

At MIT-Bates, an experiment^{34,35} is in preparation to measure parity violation in elastic electron-proton scattering at backward angles. In this case the asymmetry depends upon the elastic electromagnetic formfactors F_1^γ, F_2^γ , and the neutral weak formfactors F_1^Z, F_2^Z . The latter one is related to the proton anomalous moment coupling to the neutral weak current. In the Standard Model, and invoking strong isospin symmetry, F_2^Z is related to the electromagnetic formfactors as

$$F_2^Z = \left(\frac{1}{2} - \sin^2 \theta_W\right) F_2^\gamma - \frac{1}{4} F_2^o,$$

where F_2^o is a singlet piece which arises from equal contributions of all three quark flavors, and is therefore sensitive to the $s\bar{s}$ contributions to the proton structure³⁶. Large $s\bar{s}$ contributions to the nucleon structure are suggested by the most straight forward analysis of the EMC spin-dependent structure function measurement, and an analysis³⁷ of the pion-nucleon sigma term ($\Sigma_{\pi N}$). The parity violating asymmetry in elastic ep scattering is given by:

$$A_{pv} = -\frac{G_F Q^2}{\sqrt{2} \pi \alpha \xi}.$$

$$\begin{aligned} & [2\tau t g^2 \frac{\theta}{2} (F_1^\gamma + F_2^\gamma)(F_1^Z + F_2^Z) + (F_1^\gamma F_1^Z + \tau F_2^\gamma F_2^Z) \\ & - \frac{(E + E')}{2M_N} t g^2 \frac{\theta}{2} (1 - 4\sin^2 \theta_W) G_1 (F_1^\gamma + F_2^\gamma)], \end{aligned}$$

where $\xi = F_1^{\gamma 2} + \tau F_2^{\gamma 2} + 2\tau t g^2 \frac{\theta}{2} (F_1^\gamma + F_2^\gamma)^2$. At large electron scattering angles the first term dominates. The term with G_1 is suppressed since $(1 - 4\sin^2 \theta_W)$ is small. Since $F_1^Z \ll F_2^Z$, the asymmetry is essentially proportional to F_2^Z , and the term of interest F_2^o can immediately be extracted. The experimental setup is very similar to the one previously used in a parity violation experiment at Mainz³⁸.

4. DRELL-HEARN GERASIMOV SUM RULE.

The result of the polarized proton structure functions measurement has triggered new interest³² in experimental tests of the sum rule of Drell, Hearn³⁹ and Gerasimov⁴⁰:

$$\int_{\nu_{th}}^{\infty} \frac{d\nu}{\nu} [\sigma_{1/2}(\nu, 0) - \sigma_{3/2}(\nu, 0)] = -\frac{2\pi^2 \alpha}{M^2} k^2,$$

where ν is the photon energy, $\sigma_{1/2}$ and $\sigma_{3/2}$ are the absorption cross sections for total helicity 1/2 and 3/2, and k is the anomalous magnetic moment of the target nucleon. The interpretation of the EMC results on the polarized proton structure functions in terms of the Ellis-Jaffe sum rule suggests

$$\int_{\nu_{th}}^{\infty} \frac{d\nu}{\nu} [\sigma_{1/2}(\nu, Q^2) - \sigma_{3/2}(\nu, Q^2)] \simeq \frac{0.2}{Q^2} \cdot \left(\frac{3\pi^2 \alpha}{M^2}\right)$$

It has pointed out³⁸ that dramatic changes in the helicity structure of the γp coupling must occur when going from the deep inelastic region to $Q^2 = 0$, if the DHG sum rule were to be fulfilled. Indications that such changes of the helicity structure may indeed occur have been found in the analysis of pion photo- and electroproduction for specific resonances²². The sum rule has been derived on rather general grounds but has never been tested experimentally. An analysis of single pion production experiments places some limits on how much this sum rule may be violated⁴¹. By using a circularly polarized tagged photon beam, and polarized NH_3 as a target material, the total absorption cross section difference $\sigma_{1/2} - \sigma_{3/2}$ can directly be measured as a function of the photon energy. The integral is weighted by $1/\nu$, therefore the lower energy regime, in particular the resonance region gives the largest contributions. Medium energy machines are therefore the appropriate instruments for testing this sum rule.

5. KAON PRODUCTION ON PROTONS

At CEBAF a program to study the reaction $\gamma p \rightarrow K^+ Y$ ($Y = \Lambda, \Lambda^*, \Sigma, \Sigma^*$), and hyperon radiative decays is in preparation^{47,48}. These reactions have been poorly studied in the past. Consequently, the production mechanism is not well understood. If one takes a diagrammatic approach, one can hope to extract information about the KAN and KAN^* coupling constants. Coupling constants, extracted from photoproduction data and from hadronic data disagree. Recent calculations⁴² indicate that measurement of the Λ recoil polarization are very sensitive to specific ingredients of the model, in particular on assumptions about

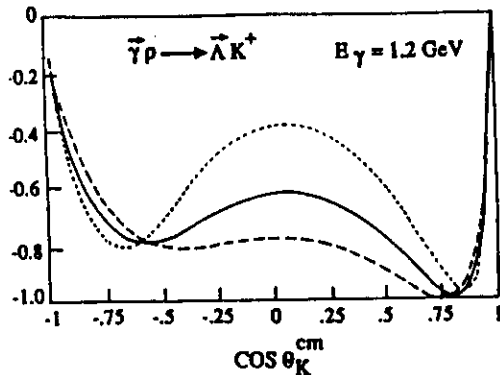


Figure 5.1 Prediction of double polarization asymmetry for $\bar{\gamma}p \rightarrow K^+\bar{\Lambda}$. The coupling constant $g_{\Lambda K}$ has been varied by +10% (dotted) and -10% (dashed). Calculations by Adelseck⁴².

the coupling constants (Figure 5.1). An efficient experimental program to study polarization degrees of freedom in the $K\Lambda$ channel requires use of large acceptance detectors with nearly 4π solid angle coverage. At CEBAF such a detector is under construction for one of the three experimental endstations. With such an instrument, detailed polarization data can be obtained for this reaction. For example, the Λ polarization can be inferred from an analysis of its π^-p decay. Using a longitudinally polarized electron beam, circularly polarized bremsstrahlung photons can be generated, and the polarization transfer reaction $\bar{\gamma}p \rightarrow K\bar{\Lambda}$ can be studied as well.

Measurement of hyperon radiative decays yields information about the quark wave function of the hyperon states. At present, radiative widths even of some of the lower mass hyperon states are either not, or only very poorly known (Figure 5.2). Using an energy tagged photon beam low mass hyperon states can be identified in the missing mass spectrum $\gamma p \rightarrow K^+X$ (Figure 5.3).

Very little electroproduction data is available on $ep \rightarrow eK^+\Lambda$, or $ep \rightarrow eK^+\Lambda^*(1520)$. In fact, there is no data available in the resonance region or near threshold. As a consequence, the reaction is theoretically not well understood. The process may be used to obtain information about the K^+ and $K^*(892)$ formfactors. An intriguing problem is presented by the $f_0(975)$. The state does not fit into the standard $q\bar{q}$ scheme for mesons. It is considered a candidate for an exotic $q\bar{q}q\bar{q}$ state, or a $(q\bar{q})(q\bar{q})$ molecule. If the $f_0(975)$ is a weakly bound mesonic molecule a strong t dependence may be expected in electromagnetic production. Using the CLAS detector at a luminosity of $10^{34} \text{ cm}^{-2} \text{ sec}^{-1}$ the number

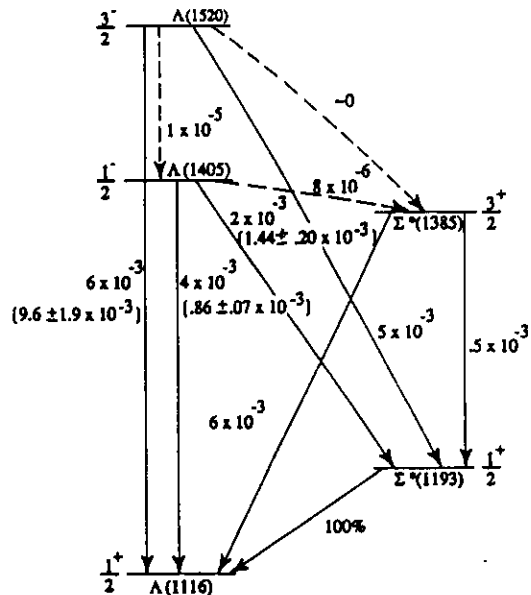


Figure 5.2 Radiative transition of low mass hyperons. The numbers indicate predicted and measured transition probabilities.

of detected f_0 events in $ep \rightarrow epK^+K^-$ is about 10^4 per day⁴³. With such a rate detailed studies of the momentum transfer dependence of the production process will be possible.

6. KAON PRODUCTION ON DEUTERIUM

In a nuclear system, the hyperon may be viewed as a controlled impurity which is unrestricted by the Pauli principle. It also lives long enough to sample the nuclear interior. These properties are used in the field of experimental hypernuclear physics. For the case of the deuterium, hyperon production can be used to study YN interactions by studying the processes $\gamma D \rightarrow K^+(\Lambda n)$, and $\gamma D \rightarrow K^+(\Sigma n)$. At CEBAF an experiment is in preparation to measure this process⁴⁹. The cross section for this process is expected to be strongly enhanced over the quasi-free production mechanism. The interference structure due to $\Lambda N \rightarrow \Sigma N$ allows to determine the relative sign of the amplitudes.

As the photon energy crosses the $N\Sigma$ threshold a sharp structure is predicted to emerge⁴⁵. In the vicinity of this cusp, two $S=-1$ dibaryon states are predicted to occur⁴⁶. The lower mass D_0 is predicted to be narrow, and may show up in the missing mass plot of $\gamma D \rightarrow K^+X$ (Figure 6.1). Note that this state cannot be produced in (K,π) or (π,K) reactions.

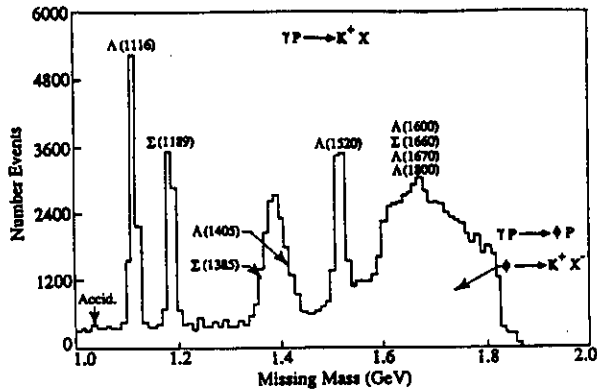


Figure 5.3 Monte Carlo simulation of the missing mass spectrum for $\gamma p \rightarrow K^+ X$ for the CEBAF Large Acceptance Spectrometer⁴⁸.

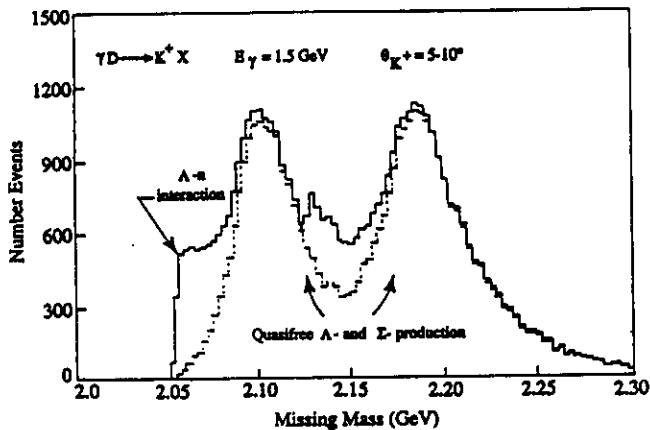


Figure 6.1 Monte Carlo simulation of $\gamma D \rightarrow K^+ X$ for the CLAS detector⁴⁹.

7. SUMMARY

I have attempted to demonstrate with a few examples of planned experiments the potential of the new DC electron machines to precisely measure photo- and electroproduction of hadrons. These reactions can teach us much about the fundamental interaction underlying the spectroscopy and internal structure of baryons and mesons. Experimental emphasis will be on precision measurements, and polarization will play a very important role in achieving this precision. Hopefully, this will also bring new challenges to theorists working in the field of strong interaction physics at intermediate energies.

I wish to thank D. Joyce and B. Mecking for discussions and useful comments, and J. Martz for preparing

the numerous graphs. I also wish to thank the organizers of the workshop for a most enjoyable and informative time in St. Goar.

REFERENCES.

- [1] S. Galster et al., Nucl. Phys. B32, 221 (1971).
- [2] S. Platchkov et al., Nucl. Phys. A510, 740 (1990).
- [3] R.G. Arnold et al., Phys. Rev. Lett. 57, 174 (1986)
- [4] M. Gari, N. Stefanis, Phys. Lett. B187, 401 (1987)
- [5] N. Dombey, Rev. Mod. Phys. 41, 236 (1969)
- [6] R. Arnold, C. Carlson, F. Gross, Phys. Rev. C23, 363 (1981)
- [7] V.D. Burkert, Lecture Notes in Physics 234, 228 (1984)
- [8] T. Reichelt, private communication (1990)
- [9] D. Day, private communication (1990)
- [10] E.W. Otten, Lecture presented at the Erice Summer School (1989).
- [11] H. Arenhovel, W. Leidemann, and E.L. Tomusiak, Z. Phys. A331, 123 (1988)
- [12] B. Blankleider and R.M. Woloshyn, Phys. Rev. C29, 538 (1984); U. Meissner, Phys. Rev. Lett. 62, 1013 (1989).
- [13] C. Perdrisat, private communications.
- [14] V. Burkert, Workshop on Electronuclear Physics with Internal Beams and Targets, SLAC (1987).
- [15] D. Crabb, University of Michigan Preprint, HE 89-31 (1989)
- [16] E.P. Mazzucato et al., Phys. Rev. Lett. 57, 3144 (1986)
- [17] R. Beck, Dissertation Thesis, Mainz, (1989).
- [18] L.M. Nath and S.K. Singh, Phys. Rev. C39, 1207 (1989)
- [19] L. Tiator and D. Drechsel, Proc. Few Body Conference, Vancouver, Canada, July (1989).
- [20] M.I. Adamovitch, Proc. P.N. Lebedev Physics Institute 71, 119(1976)
- [21] J. Spuller et al., Phys. Lett. B67, 479 (1977)
- [22] V. Burkert, 'Light Quark Baryons', these proceedings.
- [23] W. Warns et al., Z. Phys. C45, 613(1990); Z. Phys. C45, 627(1990)
- [24] C.E. Carlson and J.L. Poor, Phys. Rev. D38, 2758 (1988)
- [25] N. Isgur and G. Karl, Phys. Lett. 72B, 109 (1977); Phys. Rev. D23, 817 (1981)
- [26] I. Koniuk and N. Isgur, Phys. Rev. D21, 1868 (1980)
- [27] C.E. Carlson, Phys. Rev. D34, 2704 (1986)
- [28] R. Lourie, (Spokesman), Bates PR 89-03; C. Papanicolas (Spokesman), Bates PR 87-09

- [29] V. Burkert and R. Minchert (Spokesmen), CEBAF PR-89-37, PR-89-42
- [30] G. Kroesen and B. Boden, Research Program at CEBAF II, Summer Study Group, Newport News (1986).
- [31] Z. Li, F.E. Close, Rutherford preprint, RAL-90-010 (1990).
- [32] F.E. Close, Invited talk at the CEBAF Summer Workshop, Newport News, 1988.
- [33] R.W. Lourie, Phys. Rev. D (1990).
- [34] E. Beise et al., Bates Proposal 89-06 (1989)
- [35] R.D. McKeown, Phys. Lett. 219, 140 (1989)
- [36] D. Kaplan and A. Monahan, Nucl.Phys.B310,527 (1988)
- [37] R.L. Jaffe and C.L. Korpa, Comments Nucl. Part. Phys. 17, 103 (1987)
- [38] W. Heil et al, Nucl. Phys. B327, 1 (1989)
- [39] S.D. Drell and A.C. Hearn, Phys. Rev. Lett. 16, 908 (1966)
- [40] S. Gerasimov, Sov. J. Nucl. Phys. 2, 930 (1966)
- [41] I. Karliner, Phys. Rev. D7, 2717 (1973)
- [42] R.A. Adelseck and B. Saghai, Report DPh-N/Saclay 2544B (1989).
- [43] L. Dennis and H. Funsten (Spokesmen), CEBAF Proposal PR-89-43
- [44] M. Arguilar-Benitez et al., Particle Data Group, (1988).
- [45] S.R. Cotanch, Proc. Conf. on Medium and High Energy Nuclear Physics, Taipei, May, 1989.
- [46] C.B. Dover, Nucl. Phys. A450, 95 (1986); M.P. Locher et al., Adv. Nucl. Phys. 17, 47 (1987)
- [47] R. Schumacher (spokesman), CEBAF PR-89-4
- [48] G. Mutchler (spokesman), CEBAF PR-89-24
- [49] B. Mecking (spokesman), CEBAF PR-89-45
- [50] E. Oset, R. Tegen and W. Weise, Preprint TRP-84-1, University of Regensburg, W. Germany.
- [51] W. Konen and H.J. Weber, University of Virginia Preprint, UVa-INPP-89-6 (1989)
- [52] U.G. Meissner, N. Kaiser and W. Weise, Nucl. Phys. A466, 685 (1987)
- [53] R. Madey, private communications (1990).